Received: 9 February 2023 | Revised: 24 August 2023 | Accepted: 5 February 2024

DOI: 10.1002/mgg3.2399

Molecular Genetics & Genomic Medicine Open Access WILEY

ORIGINAL ARTICLE

Clinical report and genetic analysis of rare premature infant nephronophthisis caused by biallelic *TTC21B* variants

Yingying Li[1] | **Liying Dai**[2] | **Hong Xu**[1] | **Jin Huang**[1] | **Jinqiu Zhang**[1] | **Zhenzhu Mei**[1] | **Rui Zhang**[1]

[1]Department of Neonatology, Suzhou Hospital of Anhui Medical University (Suzhou Municipal Hospital of Anhui Province), Suzhou, Anhui, China

[2]Department of Neonatology, Anhui Province Children's Hospital, Hefei, Anhui, China

Correspondence
Yingying Li, Department of Neonatology, Suzhou Hospital of Anhui Medical University (Suzhou Municipal Hospital of Anhui Province), Suzhou, Anhui, China.
Email: liyingying210@163.com

Liying Dai, Department of Neonatology, Anhui Province Children's Hospital, Hefei, Anhui, China.
Email: anhuidailiying@163.com

Abstract

Background: Nephronophthisis (NPHP) is a genetically heterogeneous disease that can lead to end-stage renal disease (ESRD) in children. The *TTC21B* variant is associated with NPHP12 and mainly characterized by cystic kidney disease, skeletal malformation, liver fibrosis, and retinopathy. Affected patients range from children to adults. Some patients experience ESRD in infancy or early childhood, but clinical reports on neonatal patients are rare. We report a case of NPHP12 in a premature infant and analyze its genetic etiology.

Methods: Trio-whole exome sequencing analysis was performed on the patient and her parents; bioinformatics software was used to predict and analyze the hazards of the variants. Sanger sequencing was performed to verify variants. We calculated the free energy between mutant IFT139 and the IFT121-IFT122-IFT43 complex structure using molecular dynamics (MD). Finally, the clinical and genetic characteristics of patients with hotspot variant Cys518Arg were reviewed.

Results: Genetic analysis revealed compound-heterozyous TTC21B variants in the patient, c.497delA (p.Lys166fs*36) and c.1552T>C (p.Cys518Arg). Her father and mother had heterozygous c.497delA (p.Lys166fs*36) and heterozygous c.1552T>C (p.Cys518Arg), respectively. Cys518Arg represents a hotspot variant, and the MD calculation results show that this can reduce the structural stability of the IFT121-IFT122-IFT139-IFT43 complex structure. A literature review showed that Cys518Arg might lead to the early occurrence of ESRD.

Conclusions: Compound-heterozygous *TTC21B* variants underlie the phenotype in this patient. Thus, Cys518Arg may be a hotspot variant in the Chinese population. Genetic testing should be recommended for NPHP in neonates and early infants.

KEYWORDS

ciliopathy, end-stage renal disease, IFT139, nephronophthisis, TTC21B

1 | INTRODUCTION

Nephronophthisis (NPHP) is a rare disease that leads to end-stage renal disease (ESRD) in children (Luo & Tao, 2018). The main clinical features of NPHP are polyuria, polydipsia, secondary enuresis, and anemia. The symptoms of NPHP are mild at onset, and ultrasound of the kidneys is normal or shows nonspecific changes such as echogenic enhancement. Upon progression to ESRD, patients show anemia and growth retardation, while renal ultrasound displays small hyperechogenic kidneys (Chung et al., 2014). NPHP is a heterogeneous genetic disorder. To date, 26 pathological genes have been identified. These genes encode proteins localizing to primary cilia in most mammalian cells (Braun & Hildebrandt, 2017; Gupta et al., 2021; Srivastava et al., 2018). Therefore, approximately 20% of patients will have extrarenal involvement, which is termed NPHP-related ciliopathies (NPHP-RC), and includes retinal pigmentation (Senior–Løken syndrome), cerebellar vermis aplasia/hypoplasia situs inversus/cardiac malformation (Joubert syndrome), and skeletal defects (Loken et al., 1961; McInerney-Leo et al., 2015; Parisi et al., 2007; Wolf, 2015).

Loss of function (LOF) variants in 26 genes have been identified to date; however, these genes only account for approximately one-third of the pathogenic factors in patients with NPHP (Srivastava et al., 2018; Wolf, 2015). Among these, *TTC21B*-encoded tetratricopeptide repeat domain 21B intraflagellar transport 139 protein (also known as intraflagellar transport 139, IFT139) plays a key role in regulating Hedgehog (Hh) signal transduction (Tran et al., 2014). Davis et al. (2011) first reported the contribution of biallelic *TTC21B* variant in NPHP; moreover, approximately 60 cases of NPHP, or NPHP-RC associated with it, have been reported (Bezdíčka et al., 2021; Bullich et al., 2017; Chen et al., 2022; Doreille et al., 2021; Gambino et al., 2021; Halbritter et al., 2013; Huynh Cong et al., 2014; Jian et al., 2019; Kang et al., 2016; Liu et al., 2022; Otto et al., 2011; Schueler et al., 2016; Zhang et al., 2018, 2022).

The onset of NPHP in infancy is rare and usually caused by variants in *INVS* and *NPHP3* (Otto et al., 2003; Tory et al., 2009). Here, we provide a clinical report and genetic analysis of a premature patient with NPHP caused by compound-heterozygous TTC21B variants. The present report provides pathogenic evidence of the *TTC21B* variant in younger patients and provides new insight into the disease phenotype and genotype spectrum.

2 | METHODS

2.1 | Editorial policies and ethical considerations

The present study was approved by the Ethics Committee of Suzhou Hospital of Anhui Medical University (ethics batch number: 2019063). The patient is from a nonconsanguineous Chinese family. The patients' parents signed an informed consent form.

2.2 | Whole-exome sequencing and sanger sequencing

Trio-whole-exome sequencing (trio-WES) was performed on the patient and her parents, who were in a nonconsanguineous marriage. After 3 mL of peripheral blood (EDTA tube anticoagulation treatment) was collected, white blood cell DNA was extracted according to the operation steps of the genome extraction kit (CoWin Biosciences, Tianjin, China), and the designed sequence was captured using an Illumina Noveseq 6000 high-throughput sequencer (Illumina, San Diego, CA, USA). Variants were filtered using population sequencing databases including ExAC (www.exac.broadinstitute.org/), dbSNP (www.ncbi.nlm.nih.gov/snp), and 1000 Genomes (www.1000genomes.org). Variant effects were computationally predicted using online software tools SIFT (www.sift.bii.a-star.edu.sg), Polyphen-2 (www.genetics.bwh.harvard.edu/pph2), and MutationTaster (www.mutationtaster.org). Finally, the pathogenicity of the variant was rated following guidelines from the American College of Medical Genetics and Genomics (ACMG; Richards et al., 2015). Primers were designed using variant locations on the Ensemble database, and Sanger verification was performed using an ABI 3500XL Analyzer (Applied Biosystems, ThermoFisher Scientific, Waltham, MA, USA).

2.3 | Sequential and molecular dynamics analysis

The IFT139 protein encoded by *TTC21B* and IFT121-IFT122-IFT43 comprises the IFT-A2 complex with biological function (Hesketh et al., 2022). Therefore, we predicted and analyzed the structure of the mutant IFT139 protein and the IFT121-IFT122-IFT139-IFT43 complex. First, we downloaded the IFT121-IFT122-IFT139-IFT43 complex structure (PDB:8BBE) file from the RCSB PDB database (www.rcsb.org/structure/8BBE)

TABLE 1 Auxiliary examination information of the neonatal patient.

	Reference range	Day 1	Day 5	Day 12	Day 13	Day 16	Day 19	Day 32
HB	140–200 g/L	135	108	103	83	117 (after blood transfusion)	121 (after blood transfusion)	73
Serum potassium	3.50–5.50 mmol/L	4.15	4.58	7.76	7.28	5.80	7.89	5.96
Serum sodium	135.0–145.0 mmol/L	137.4	135.2	146.4	141.0	133.0	122.0	152.0 (after oral sodium)
Serum chlorine	98.0–106.0 mmol/L	100.4	95.3	105.4	105.0	91.0	86.0	108.5
Serum phosphorus	0.81–1.62 mmol/L	NA	NA	NA	2.33	2.65	3.52	3.33
BUN	2.0–8.2 mmol/L	3.9	NA	25.9	23.3	21.2	28.0	21.3
Cr	18.0–69.0 μmol/L	67.0	NA	362.0	356.2	384.2	386.5	386.0
Cys-C	0.59–1.03 mg/L	NA	NA	NA	4.14	5.54	4.40	4.31
Proteinuria	+/−	NA	NA	NA	NA	+	+	+
BLD	+/−	NA	NA	NA	NA	+	+	+

Abbreviations: +/−, positive/negative; BLD, urine latent blood; BUN, blood urea nitrogen; Cr, creatinine; Cys-C, cystatin C; HB, hemoglobin; NA, not available.

and constructed a mutant structure based on the wild-type structure. Molecular dynamics (MD) simulation was carried out using the Gromacs 5.14 software with the Gromos53a6 molecular force field and SPC water model for a total simulation time of 50 ns. The initial velocity of the formal MD simulation was set as the random initial velocity. The root mean square deviation (RMSD) data of the wild-type complex structure and mutant were calculated using the gmx rms tool; the visual structure diagram was drawn using PyMOL v2.5, and the curve diagram was drawn using the Origin v8.5 software.

3 | RESULTS

3.1 | Case presentation

The patient was a female neonate, G2P2, delivered by cesarean section owing to insufficient amniotic fluid at 35^{+5} weeks of gestation. The birth weight was 2380 g (−1.5 standard deviation), and there was no history of asphyxia or rescue. Her mother's routine prenatal B-ultrasound examination during pregnancy showed enhanced echogenictiy of both fetal kidneys. Physical examination after birth showed the appearance of the premature infant characterized by reddish skin; thin, messy, and soft hair; excess vellus hair growth; weak cries; shortness of breath; positive nasal fan and triple concave sign; slightly narrow chest; short fingers; and no polydactyly.

Auxiliary examination showed that liver and kidney functions and electrolytes were normal on the first day after birth, and hemoglobin (HB) was slightly low at 135 g/L (reference range: 140–200 g/L). The liver and kidney function and electrolyte levels were normal on the fifth day, and the HB value was further reduced to 108 g/L. On the 12th day, no abnormalities were observed in the liver function test. The renal function test showed that the blood urea nitrogen (BUN) was abnormally increased (25.9 mmol/L, reference range: 2.0–8.2 mmol/L), creatinine (Cr) value was abnormally increased (398 μmol/L, reference range: 18–69 μmol/L) owing to an electrolyte disorder, and HB was further reduced to 83 g/L. On the 16th day, the results were 24-h urine microalbumin 230.7 mg/L (reference range: <30.0 mg/L) and β_2 microglobulin 23.600 mg/L (reference range: 0.016–0.518 mg/L). On the 19th day, the BUN and Cr values remained abnormally high and the electrolytes were disordered (Table 1). B-ultrasound of the urinary system showed diffuse renal lesions on both sides and separation of the right renal pelvis. Chest radiography showed some irregularly shaped ribs (Figure 1). Cardiac B-ultrasound showed patent foramen ovale and patent ductus arteriosus. Brain ultrasound showed brain changes in the premature infant, mainly immature brain development, and an electrocardiogram showed sinus tachycardia.

The patient was transferred to another hospital for intervention 30 days after birth. HB continued to decrease, anemia symptoms were progressive, serum creatinine enzyme and serum phosphorus levels increased, and renal B-ultrasound showed parenchymal damage in both kidneys. The glomerular filtration rate (GFR) value was 4.73 mL/(min/1.73 m^2; referring to the KDIGO organization guide standard, the ESRD phase GFR was <15.00 mL/[min/1.73 m^2]; Radhakrishnan & Cattran, 2012). Subsequently, the patient's parents discontinued treatment and did not complete renal biopsy for pathological examination. The patient died at the age of 3 months. The patient's parents and 9-year-old brother are healthy.

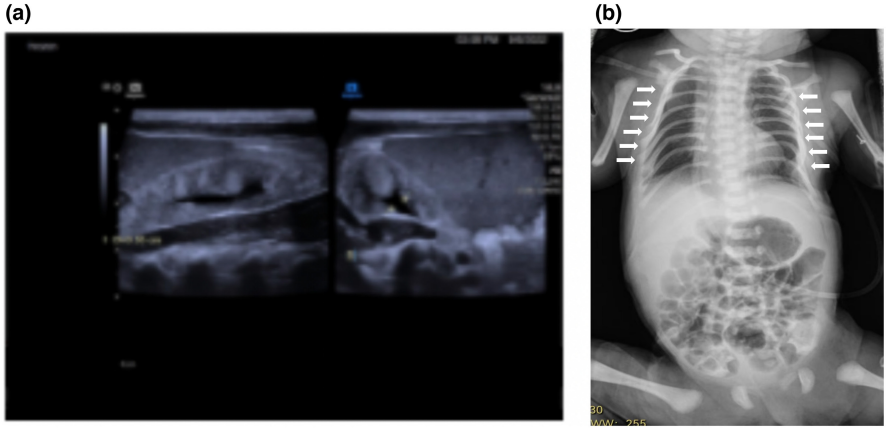

FIGURE 1 Imaging characteristics of the patient. (a) Renal ultrasound reveals diffuse lesions in both kidneys and separation of the right renal pelvis. (b) Radiographic examination shows irregular ribs (see arrows).

3.2 | Gene test results

WES suggested that the patient had compound-heterozygous *TTC21B* variants, NM_024753.5: c.497delA/p.Lys166fs*36 and c.1552T>C/p.Cys518Arg. The father carried heterozygous c.497delA/p.Lys166fs*36 and the mother carried heterozygous c.1552T>C/p.Cys518Arg. These two variants were not included in the dbSNP, ExAC, or 1000 Genomes databases. The c.497delA/p.Lys166fs*36 is a predicted LOF variant of *TTC21B* that introduces a premature termination codon within an exon and may trigger nonsense-mediated mRNA decay. In addition, the variant is not present in population sequencing databases and is therefore rated as likely pathogenic (PVS1+PM2_Supporting) according to ACMG guidelines. Another variant, c.1552T>C/p.Cys518Arg, has been detected in several phenotype-related patients. The predicted hazard value of the SIFT algorithm was 0.001 (damaging), Polyphen2_HDIV was 0.981 (damaging), Polyphen2_HVAR was 0.963 (damaging), and MutationTaster was 1 (disease-causing). According to the ACMG guidelines, it is rated as likely pathogenic (PM2_Supporting+PM3_Strong+PP3). Sanger sequencing confirmed the presence of compound-heterozygous *TTC21B* variants. The patient's parents were heterozygous carriers, and the brother was wild-type (Figure 2).

3.3 | Mutant Cys518Arg may affect the structural stability of IFT121-IFT122-IFT139-IFT43 complex

According to the RMSD monitoring of the average deviation between the structure of the wild-type IFT121-IFT122-IFT139-IFT43 complex and the mutant, the corresponding RMSD values when the wild-type and mutant simultaneously reach the equilibrium state are approximately 2.75 Å and 2.70 Å, respectively. In the wild-type system, the Cys518 in IFT139 has no polarity with the surrounding residues, while the mutant Cys518Arg leads to the formation of a new hydrogen bond between Arg518 and Leu492, which may result in changes in the stability of local outcomes. Structural analysis of the IFT121-IFT122-IFT139-IFT43 complex showed that the mutant IFT139 protein (Cys518Arg) led to the formation of a new hydrogen bond between Lys705 of IFT139 and Glu1095 of IFT122, which may enhance the interaction between proteins (Figure 3). The results of free binding energy analysis showed that the total free binding energy of the wild-type IFT121-IFT122-IFT139-IFT43 complex (−141.33 kJ/mol) was lower than that of the mutant type (−203.19 kJ/mol), and the main difference was the van der Waals force (Table 2). Therefore, the mutant IFT139 protein Cys518Arg may reduce the structural stability of the IFT121-IFT122-IFT139-IFT43 complex, thereby affecting its biological function.

4 | DISCUSSION

Here, we report the clinical information of a neonatal patient with NPHP. The patient was a 35^{+5} weeks premature infant. Her mother's routine prenatal ultrasound examination showed enhanced echogenicity of both fetal kidneys. The patient had neonatal anemia, but no abnormal liver and kidney function after birth. On the 12th day, the patient developed abnormal renal function and electrolyte disorder, followed by the symptoms of proteinuria and occult hematuria. The patient's renal disease progressed rapidly, and she developed ESRD on the 30th day after birth. Symptoms of anemia gradually worsened. In addition to renal manifestations, the patient also had congenital heart disease with patent foramen ovale, patent ductus arteriosus, and irregular ribs. Whole-exome sequencing showed that this patient had compound-heterozygous *TTC21B* variants of Lys166fs*36 and Cys518Arg. Therefore, the NPHP and extrarenal clinical features of this patient may have been caused by the compound-heterozygous *TTC21B* variants and was finally diagnosed as NPHP12 (OMIM # 613820).

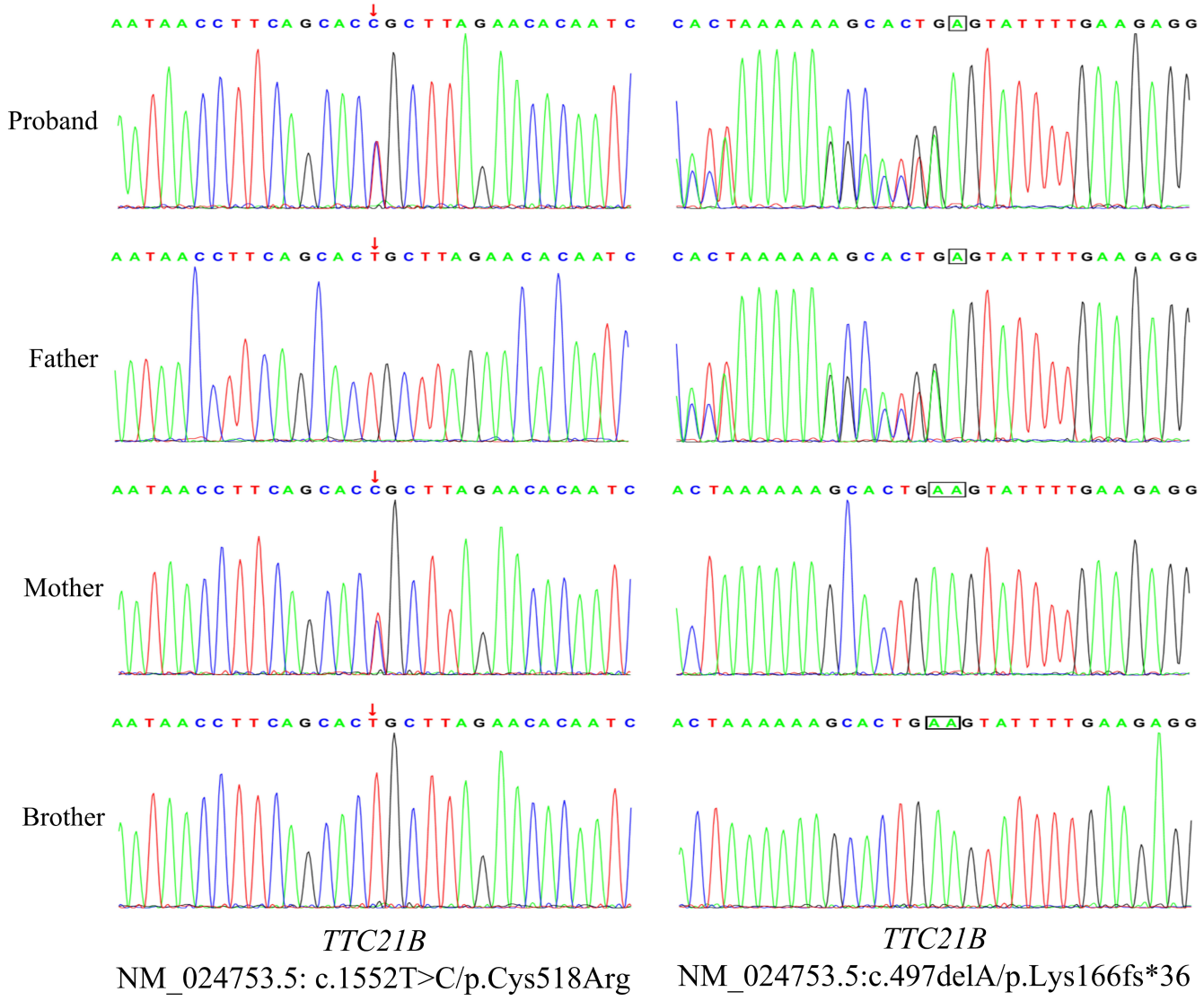

FIGURE 2 Genetic detection results suggest that the patient had compound-heterozygous *TTC21B* variants, c.497delA (p.Lys166fs*36) and c.1552T>C (p.Cys518Arg). The father carried heterozygote c.497delA (p.Lys166fs*36), the mother carried heterozygote c.1552T>C (p.Cys518Arg), and the brother was wild-type.

TTC21B is located on chromosome 2q24.3, has 29 exons across the domain, and consists of 1316 amino acids that form the IFT139 protein. The IFT is a macromolecular complex composed of IFT-A and IFT-B and is responsible for the bidirectional transport of axonal microtubules in the cilia (Jordan et al., 2018). The IFT-A complex comprises IFT-A1 and IFT-A2, connected by flexible areas. The IFT-A2 structure is relatively stable (Hirano et al., 2017). Recently published research results further revealed that IFT-A1 has three axial motion processes relative to IFT-A2; therefore, it is very important for the structural stability of IFT-A2. The IFT-A2 structure comprises IFT121-IFT122-IFT139-IFT43. IFT139 and IFT43 play key roles in the stability of the IFT-A2 structure and can maintain the flexibility of IFT-A1, consequently contributing to the polymerization process of the IFT-A complex (Hesketh et al., 2022).

The mutant Cys518Arg reported in the present study occurred in the tetratricopeptide repeat 6 region of the IFT139 protein, which may form a new hydrogen bond with Leu492, resulting in changes in local structural stability. Simultaneously, the IFT139 mutant proteins interact with IFT122. According to the calculation results of the free binding energy, the mutant IFT121-IFT122-IFT139-IFT43 complex has higher energy than the wild-type, which indicates that the structural stability of the mutant complex may be reduced, thus potentially affecting biological functions. Another variant, Lys166fs*36, is a rare predicted LOF variant, which provides strong evidence for pathogenicity. This variant has not been reported and is

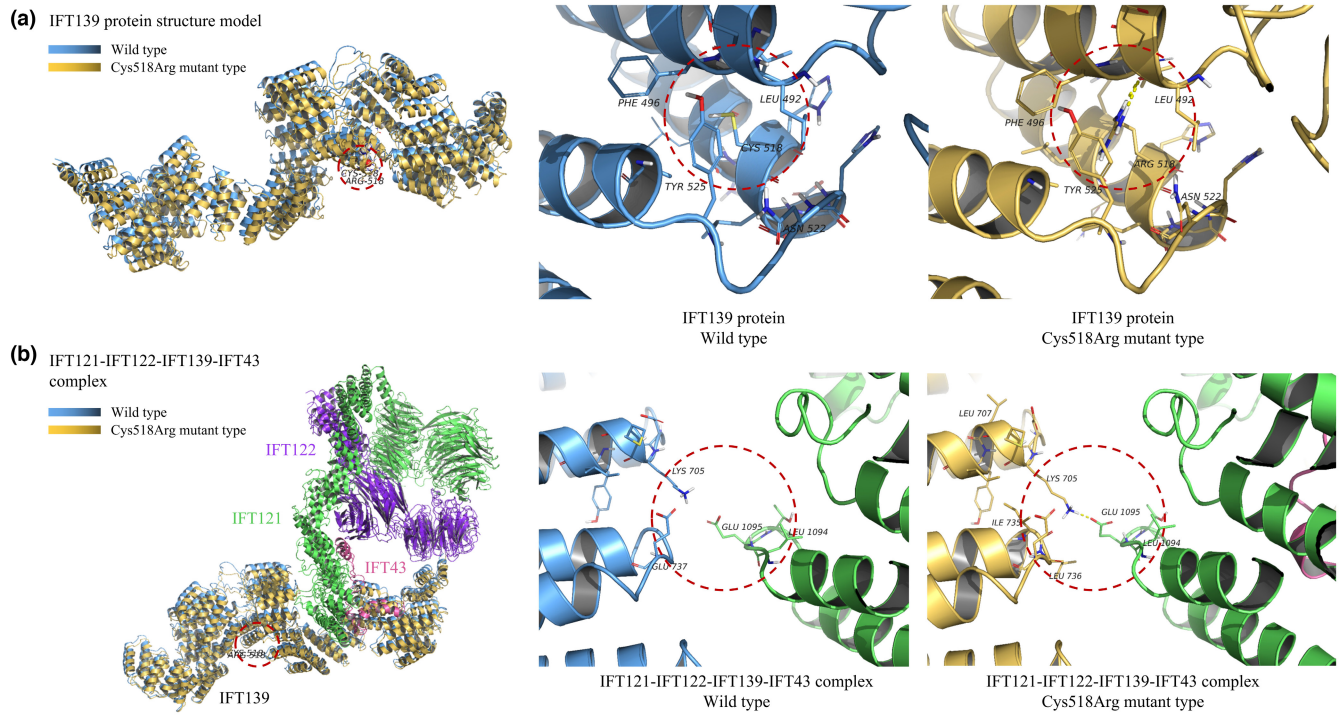

FIGURE 3 Protein structure prediction analysis results. (a) Cys518 in the wild-type IFT139 protein (encoded by *TTC21B*) does not form a polar bond with the surrounding residues. Cys518Arg can lead to the formation of a new hydrogen bond (location indicated by the red circle) between Arg518 and Leu492, which may lead to changes in the local structural stability and even affect the structural stability of the IFT121-IFT122-IFT139-IFT43 complex. (b) Mutant IFT139 protein (Cys518Arg) causes the Lys705 residue of IFT139 to form a new hydrogen bond with the Glu1095 of IFT122; the new interaction between proteins may lead to reduced structural stability of the IFT121-IFT122-IFT139-IFT43 complex, thereby affecting biological function (the red circle marks the location of the new hydrogen bond).

TABLE 2 Free binding energy data of wild-type/mutant IFT139 and IFT121-IFT122-IFT43 complex.

Item	Wild-type energy value (kJ/mol)	Mutant-type energy value (kJ/mol)
$\triangle E_{vdw}$	−203.18 ± 1.44	−215.48 ± 1.01
$\triangle E_{ele}$	−26.99 ± 0.56	−46.08 ± 0.45
$\triangle G_{polar}$	118.18 ± 1.21	87.58 ± 1.36
$\triangle G_{nonpolar}$	−29.34 ± 0.18	−29.21 ± 0.54
$\triangle G_{bind}$	−141.33 ± 1.44	−203.19 ± 1.66

Abbreviations: E_{ele}: Electrostatic interaction; E_{vdw}: Van Der Waals force; G_{bind}: Binding free energy; $G_{nonpolar}$: Nonpolar solvation energy; G_{polar}: Polar solvation energy.

a novel variant of *TTC21B*, which enriches the *TTC21B* gene variation spectrum.

Presently, the pathogenesis of NPHP caused by the mutant protein IFT139 is unclear; however, the IFT complex plays a key role in the localization of the Hh signal protein in the cilia. The normal Hh signaling pathway is conducive to kidney development, and its ligand Shh is the main protein expressed in the embryonic epithelial cells at the distal end of the ureter and medullary collecting duct (Hu et al., 2006). Tran et al. (2014) also confirmed that the IFT139 protein could regulate the Hh signal transduction process. Therefore, the decreased function of the IFT139 protein may interfere with the effect of the Hh signaling pathway on kidney development owing to the influence of the IFT complex biological function.

There may be a correlation between the *TTC21B* genotype and phenotype. Different variant sites or types exhibit phenotypic differences. However, patients generally exhibit elevated creatinine levels and proteinuria. The pathological manifestation of the renal disease was interstitial nephritis. The main phenotypic differences are reflected in the speed and severity of renal disease progression (Bezdíčka et al., 2021; Bullich et al., 2017; Chen et al., 2022; Davis et al., 2011; Doreille et al., 2021; Gambino et al., 2021; Halbritter et al., 2013; Huynh Cong et al., 2014; Jian et al., 2019; Kang et al., 2016; Liu et al., 2022; Otto et al., 2011; Schueler et al., 2016; Zhang et al., 2018, 2022). The *TTC21B* variant Cys518Arg, elucidated in the present study, has been reported many times in previous patients and is one of the hotspots. Eleven patients (4 male and 7 female) were found to carry the Cys518Arg variant in eight Chinese NPHP families (Chen et al., 2022; Jian et al., 2019; Liu

TABLE 3 Clinical and genetic information of patients with *TTC21B* variant Cys518Arg.

Patient	Sex	Age of onset	ESRD	Clinical characteristics	Mutation information	References
1	F	1 year	1 year	Edema, hypertension, proteinuria, hypoproteinemia, hyperlipidemia, anemia, renal function damage, liver function abnormality. Renal ultrasound: boundary between the cortex and medulla is unclear, and echo is enhanced	c.1552T>C/c.1456dupA; p.Cys518Arg/p.Arg486fsX	Zhang et al. (2018)
2	M	6 years	6 years	Kidney consumption-related syndrome and visceral inversion, no structural abnormality of the heart	c.1552T>C/c.1656_1659del; p.Cys518Arg/p.Cys552fsX	Chen et al. (2022)
3	F	1 year	1 year	Cholestasis, hyperlipidemia, chronic kidney disease, liver function damage	c.1552T>C/c.1656_1659del; p.Cys518Arg/p.Cys552fsX	–
4	F	3 years	4 years	Hypertension, proteinuria, renal insufficiency, heart failure, anemia, specular dextrocardia. Abdominal ultrasound: whole visceral transposition, diffuse enhancement of echo in both renal parenchyma, unclear boundary between skin and marrow	c.1552T>C/c.752T>G; p.Cys518Arg/p.Met251Arg	Jian et al. (2019)
5	F	16 years	16 years	Hypertension, anemia, renal insufficiency, elevated parathyroid hormone. Abdominal ultrasound: hyperechogenicity of kidney	c.1552T>C/c.2309A>G; p.Cys518Arg/p.His770Arg	Liu et al. (2022)
6	F	28 months	38 months	Anemia, hypertension, impairment of liver and kidney function, proteinuria. Renal ultrasound: small kidney volume, enhanced echo of parenchyma, and visceral inversion	c.1552T>C/c.1231C>T; p.Cys518Arg/p.Arg411X	Zhang et al. (2022)
7	M	25 months	25 months	Hypertension, proteinuria, liver, and kidney function damage. Abdominal ultrasound: small size of both kidneys with diffuse changes, hepatomegaly with diffuse changes	c.1552T>C/c.1231C>T; p.Cys518Arg/p.Arg411X	–
8	M	16 months	48 months	Hypertension, anemia, proteinuria, liver and kidney function damage. Abdominal ultrasound: no abnormality in both kidneys, dextrocardia	c.1552T>C/c.1675-1G>T; p.Cys518Arg/-	–
9	F	4 months	6 months	Proteinuria, renal function damage	c.1552T>C/c.1675-1G>T; p.Cys518Arg/-	–
10	F	6 months	15 months	Hypertension, anemia, proteinuria, renal function damage	c.1552T>C/c.1327C>G; p.Cys518Arg/p.Leu443Val	–
11	M	19 months	26 months	Hypertension, anemia, proteinuria, renal function damage. Renal ultrasound: bilateral renal atrophy with diffuse changes, right lower pole cyst	c.1552T>C/c.530delA; p.Cys518Arg/p.Asp177fsX	–
Our study	F	12 days	2 months	Hyperkalemia, hyponatremia, anemia, proteinuria, renal function damage, thoracic dysplasia, diffuse renal disease	c.1552T>C/c.497delA; p.Cys518Arg/p.Lys166fsX	–

Abbreviations: ESRD, end-stage renal disease; F, female; M, male.

et al., 2022; Zhang et al., 2018, 2022). The median age of onset of these patients was 19 months, and the median age of ESRD occurrence was 3.1 years old. Most had proteinuria (primarily glomerular proteinuria) but no hematuria. The extrarenal manifestations were mainly hypertension (8/11), liver function damage (5/11), and visceral inversion (4/11); no bone abnormalities were reported. These patients had a compound-heterozygous *TTC21B* variant. Except for Cys518Arg, other variant types included frameshift variants, nonsense variants, and splice variants (Table 3). It is worth noting that the hotspot variant of *TTC21B* in North Africa and Portugal is Pro209Leu and is in the form of homozygous or compound-heterozygous variants leading to focal segmental glomerular sclerosis (FSGS), delayed proteinuria, and delayed ESRD (concentrated in the age of 15–35 years). The appearance of extrarenal involvement mainly manifests as hypertension and liver function damage (Bezdíčka et al., 2021; Bullich et al., 2017; Doreille et al., 2021; Gambino et al., 2021; Huynh Cong et al., 2014). Huynh Cong et al. (2014) found that Pro209Leu could prevent some of the disordered rearrangement with the actin cytoskeleton caused by the depletion of the IFT139 protein. In addition, Pro209Leu causes little damage to microtubule anchoring, such as separated centrioles and ectopic microtubule clusters, as well as microtubule hypermethylation (Huynh Cong et al., 2014). Therefore, these results suggest that patients with Pro209Leu are milder than those with Cys518Arg, which is mainly reflected in the development rate of renal wasting disease.

Unfortunately, there is no specific treatment for NPHP12, and symptomatic treatment is the primary method. However, these interventions only delay the progression of renal function loss and cannot prevent ESRD occurrence (Stokman et al., 2021). Renal transplantation is an effective treatment for confirmed NPHP as patients with NPHP do not experience recurrence after transplantation (Bullich et al., 2017; Huynh Cong et al., 2014; Tayfur et al., 2011). With an in-depth study of the pathogenesis of NPHP and improvements in targeted drug research and development or gene therapy, it is believed that targeted treatment strategies will improve patients' quality of life.

In conclusion, we report the clinical manifestation of a rare NPHP12 premature infant, probably the youngest NPHP12 patient to date. The results of genetic detection suggest compound-heterozygous *TTC21B* variants, including the Chinese population-specific Cys518Arg hotspot variant. Patients with Cys518Arg may have an earlier onset age and develop ESRD more rapidly. Therefore, for young patients with NPHP, regardless of family history, genetic testing should be improved as soon as possible to clarify the variant information, which provides important data support for adjusting nursing plans and family genetic counseling.

AUTHOR CONTRIBUTIONS

YL and LD wrote the main manuscript. YL, HX, and JH conducted the molecular genetics experiments. YL, JZ, ZM, and RZ prepared the clinical data. LD critically revised the manuscript. All authors reviewed, read, and approved the final manuscript.

ACKNOWLEDGMENTS

We thank the patient and her family members for taking part in this study.

FUNDING INFORMATION

This work was not supported by any funding.

CONFLICT OF INTEREST STATEMENT

All authors declare that there is no conflict of interest.

DATA AVAILABILITY STATEMENT

The data that support the findings of this study are available from the corresponding author upon reasonable request.

ETHICS STATEMENT

The work was approved by the ethics committee of the Suzhou Hospital of Anhui Medical University (ethics batch number: 2019063).

ORCID

Liying Dai https://orcid.org/0000-0002-7133-1013

REFERENCES

Bezdíčka, M., Zemková, D., Skálová, S., Hovorková, E., Podhola, M., Burkert, J., & Zieg, J. (2021). Tubuloglomerular disease with cone-shaped epiphyses associated with Hypomorphic variant and a novel p.Cys14Arg in the TTC21B gene: A case report. *Frontiers in Pediatrics*, *9*, 752878. https://doi.org/10.3389/fped.2021.752878

Braun, D. A., & Hildebrandt, F. (2017). Ciliopathies. *Cold Spring Harbor Perspectives in Biology*, *9*(3), a028191. https://doi.org/10.1101/cshperspect.a028191

Bullich, G., Vargas, I., Trujillano, D., Mendizábal, S., Piñero-Fernández, J. A., Fraga, G., García-Solano, J., Ballarín, J., Estivill, X., Torra, R., & Ars, E. (2017). Contribution of the TTC21B gene to glomerular and cystic kidney diseases. *Nephrology, Dialysis, Transplantation: Official Publication of the European Dialysis and Transplant Association—European Renal Association*, *32*(1), 151–156. https://doi.org/10.1093/ndt/gfv453

Chen, W., Wang, F., Zeng, W., Zhang, X., Shen, L., Zhang, Y., & Zhou, X. (2022). Biallelic mutations of TTC12 and TTC21B were identified in Chinese patients with multisystem ciliopathy syndromes. *Human Genomics*, *16*(1), 48. https://doi.org/10.1186/s40246-022-00421-z

Chung, E. M., Conran, R. M., Schroeder, J. W., Rohena-Quinquilla, I. R., & Rooks, V. J. (2014). From the radiologic pathology archives: Pediatric polycystic kidney disease and other ciliopathies: Radiologic-pathologic correlation. *Radiographics: A Review Publication of the Radiological Society of North America, Inc*, *34*(1), 155–178. https://doi.org/10.1148/rg.341135179

Davis, E. E., Zhang, Q., Liu, Q., Diplas, B. H., Davey, L. M., Hartley, J., Stoetzel, C., Szymanska, K., Ramaswami, G., Logan, C. V., Muzny, D. M., Young, A. C., Wheeler, D. A., Cruz, P., Morgan, M., Lewis, L. R., Cherukuri, P., Maskeri, B., Hansen, N. F., … Katsanis, N. (2011). TTC21B contributes both causal and modifying alleles across the ciliopathy spectrum. *Nature Genetics*, *43*(3), 189–196. https://doi.org/10.1038/ng.756

Doreille, A., Raymond, L., Lebre, A. S., Linster, C., Saraeva Lamri, R., Karras, A., Khayat, R., Michel, P. A., Buob, D., Luque, Y., Rafat, C., & Mesnard, L. (2021). Nephronophthisis in young adults phenocopying thrombotic microangiopathy and severe nephrosclerosis. *Clinical Journal of the American Society of Nephrology: CJASN*, *16*(4), 615–617. https://doi.org/10.2215/CJN.11890720

Gambino, G., Catalano, C., Marangoni, M., Geers, C., Moine, A. L., Boon, N., Smits, G., & Ghisdal, L. (2021). Case report: Homozygous pathogenic variant P209L in the TTC21B gene: A rare cause of end stage renal disease and biliary cirrhosis requiring combined liver-kidney transplantation. A case report and literature review. *Frontiers in Medicine*, *8*, 795216. https://doi.org/10.3389/fmed.2021.795216

Gupta, S., Ozimek-Kulik, J. E., & Phillips, J. K. (2021). Nephronophthisis-pathobiology and molecular pathogenesis of a rare kidney genetic disease. *Genes*, *12*(11), 1762. https://doi.org/10.3390/genes12111762

Halbritter, J., Porath, J. D., Diaz, K. A., Braun, D. A., Kohl, S., Chaki, M., Allen, S. J., Soliman, N. A., Hildebrandt, F., Otto, E. A., & GPN Study Group. (2013). Identification of 99 novel mutations in a worldwide cohort of 1,056 patients with a nephronophthisis-related ciliopathy. *Human Genetics*, *132*(8), 865–884. https://doi.org/10.1007/s00439-013-1297-0

Hesketh, S. J., Mukhopadhyay, A. G., Nakamura, D., Toropova, K., & Roberts, A. J. (2022). IFT-A structure reveals carriages for membrane protein transport into cilia. *Cell*, *185*(26), 4971–4985.e16. https://doi.org/10.1016/j.cell.2022.11.010

Hirano, T., Katoh, Y., & Nakayama, K. (2017). Intraflagellar transport-a complex mediates ciliary entry and retrograde trafficking of ciliary G protein-coupled receptors. *Molecular Biology of the Cell*, *28*(3), 429–439. https://doi.org/10.1091/mbc.E16-11-0813

Hu, M. C., Mo, R., Bhella, S., Wilson, C. W., Chuang, P. T., Hui, C. C., & Rosenblum, N. D. (2006). GLI3-dependent transcriptional repression of Gli1, Gli2 and kidney patterning genes disrupts renal morphogenesis. *Development (Cambridge, England)*, *133*(3), 569–578. https://doi.org/10.1242/dev.02220

Huynh Cong, E., Bizet, A. A., Boyer, O., Woerner, S., Gribouval, O., Filhol, E., Arrondel, C., Thomas, S., Silbermann, F., Canaud, G., Hachicha, J., Ben Dhia, N., Peraldi, M. N., Harzallah, K., Iftene, D., Daniel, L., Willems, M., Noel, L. H., Bole-Feysot, C., … Antignac, C. (2014). A homozygous missense mutation in the ciliary gene TTC21B causes familial FSGS. *Journal of the American Society of Nephrology: JASN*, *25*(11), 2435–2443. https://doi.org/10.1681/ASN.2013101126

Jian, S., Wei, Q. J., Liu, Y. T., Wang, W., Zhou, Y., Quan, M. Y., He, Y. Y., Song, H. M., & Wei, M. (2019). Clinical features and TTC21B genotype of a child with nephronophthisis type 12. *Chinese Journal of Contemporary Pediatrics*, *21*(6), 580–584. https://doi.org/10.7499/j.issn.1008-8830.2019.06.015

Jordan, M. A., Diener, D. R., Stepanek, L., & Pigino, G. (2018). The cryo-EM structure of intraflagellar transport trains reveals how dynein is inactivated to ensure unidirectional anterograde movement in cilia. *Nature Cell Biology*, *20*(11), 1250–1255. https://doi.org/10.1038/s41556-018-0213-1

Kang, H. G., Lee, H. K., Ahn, Y. H., Joung, J. G., Nam, J., Kim, N. K., Ko, J. M., Cho, M. H., Shin, J. I., Kim, J., Park, H. W., Park, Y. S., Ha, I. S., Chung, W. Y., Lee, D. Y., Kim, S. Y., Park, W. Y., & Cheong, H. I. (2016). Targeted exome sequencing resolves allelic and the genetic heterogeneity in the genetic diagnosis of nephronophthisis-related ciliopathy. *Experimental & Molecular Medicine*, *48*(8), e251. https://doi.org/10.1038/emm.2016.63

Liu, L., Li, F., Zou, H., He, W., Zhang, B., & Zhang, J. (2022). A case of proliferative glomerulosclerosis with compound heterozygous TTC21B mutations. *Clinica Chimica Acta; International Journal of Clinical Chemistry*, *529*, 17–20. https://doi.org/10.1016/j.cca.2022.01.020

Loken, A. C., Hanssen, O., Halvorsen, S., & Jolster, N. J. (1961). Hereditary renal dysplasia and blindness. *Acta Paediatrica*, *50*, 177–184. https://doi.org/10.1111/j.1651-2227.1961.tb08037.x

Luo, F., & Tao, Y. H. (2018). Nephronophthisis: A review of genotype-phenotype correlation. *Nephrology (Carlton, Vic.)*, *23*(10), 904–911. https://doi.org/10.1111/nep.13393

McInerney-Leo, A. M., Harris, J. E., Leo, P. J., Marshall, M. S., Gardiner, B., Kinning, E., Leong, H. Y., McKenzie, F., Ong, W. P., Vodopiutz, J., Wicking, C., Brown, M. A., Zankl, A., & Duncan, E. L. (2015). Whole exome sequencing is an efficient, sensitive and specific method for determining the genetic cause of short-rib thoracic dystrophies. *Clinical Genetics*, *88*(6), 550–557. https://doi.org/10.1111/cge.12550

Otto, E. A., Ramaswami, G., Janssen, S., Chaki, M., Allen, S. J., Zhou, W., Airik, R., Hurd, T. W., Ghosh, A. K., Wolf, M. T., Hoppe, B., Neuhaus, T. J., Bockenhauer, D., Milford, D. V., Soliman, N. A., Antignac, C., Saunier, S., Johnson, C. A., Hildebrandt, F., & GPN Study Group. (2011). Mutation analysis of 18 nephronophthisis associated ciliopathy disease genes using a DNA pooling and next generation sequencing strategy. *Journal of Medical Genetics*, *48*(2), 105–116. https://doi.org/10.1136/jmg.2010.082552

Otto, E. A., Schermer, B., Obara, T., O'Toole, J. F., Hiller, K. S., Mueller, A. M., Ruf, R. G., Hoefele, J., Beekmann, F., Landau, D., Foreman, J. W., Goodship, J. A., Strachan, T., Kispert, A., Wolf, M. T., Gagnadoux, M. F., Nivet, H., Antignac, C., Walz, G., … Hildebrandt, F. (2003). Mutations in INVS encoding inversin cause nephronophthisis type 2, linking renal cystic disease to the function of primary cilia and left-right axis determination. *Nature Genetics*, *34*(4), 413–420. https://doi.org/10.1038/ng1217

Parisi, M. A., Doherty, D., Chance, P. F., & Glass, I. A. (2007). Joubert syndrome (and related disorders) (OMIM 213300). *European Journal of Human Genetics: EJHG*, *15*(5), 511–521. https://doi.org/10.1038/sj.ejhg.5201648

Radhakrishnan, J., & Cattran, D. C. (2012). The KDIGO practice guideline on glomerulonephritis: Reading between the (guide)lines—Application to the individual patient. *Kidney International*, *82*(8), 840–856. https://doi.org/10.1038/ki.2012.280

Richards, S., Aziz, N., Bale, S., Bick, D., Das, S., Gastier-Foster, J., Grody, W. W., Hegde, M., Lyon, E., Spector, E., Voelkerding, K., Rehm, H. L., & ACMG Laboratory Quality Assurance Committee. (2015). Standards and guidelines for the interpretation of sequence variants: A joint consensus recommendation of the American College of Medical Genetics and Genomics and the Association for Molecular Pathology. *Genetics in Medicine: Official Journal of the American College of Medical Genetics*, *17*(5), 405–424. https://doi.org/10.1038/gim.2015.30

Schueler, M., Halbritter, J., Phelps, I. G., Braun, D. A., Otto, E. A., Porath, J. D., Gee, H. Y., Shendure, J., O'Roak, B. J., Lawson, J. A., Nabhan, M. M., Soliman, N. A., Doherty, D., & Hildebrandt, F. (2016). Large-scale targeted sequencing comparison highlights extreme genetic heterogeneity in nephronophthisis-related ciliopathies. *Journal of Medical Genetics*, *53*(3), 208–214. https://doi.org/10.1136/jmedgenet-2015-103304

Srivastava, S., Molinari, E., Raman, S., & Sayer, J. A. (2018). Many genes-one disease? Genetics of Nephronophthisis (NPHP) and NPHP-associated disorders. *Frontiers in Pediatrics*, *5*, 287. https://doi.org/10.3389/fped.2017.00287

Stokman, M. F., Saunier, S., & Benmerah, A. (2021). Renal ciliopathies: Sorting out therapeutic approaches for nephronophthisis. *Frontiers in Cell and Developmental Biology*, *9*, 653138. https://doi.org/10.3389/fcell.2021.653138

Tayfur, A. C., Besbas, N., Bilginer, Y., Ozaltin, F., Duzova, A., Bakkaloglu, M., Aki, F. T., Ozen, S., Topaloglu, R., & Bakkaloglu, A. (2011). Follow-up of patients with juvenile nephronophthisis after renal transplantation: A single center experience. *Transplantation Proceedings*, *43*(3), 847–849. https://doi.org/10.1016/j.transproceed.2011.01.107

Tory, K., Rousset-Rouvière, C., Gubler, M. C., Morinière, V., Pawtowski, A., Becker, C., Guyot, C., Gié, S., Frishberg, Y., Nivet, H., Deschênes, G., Cochat, P., Gagnadoux, M. F., Saunier, S., Antignac, C., & Salomon, R. (2009). Mutations of NPHP2 and NPHP3 in infantile nephronophthisis. *Kidney International*, *75*(8), 839–847. https://doi.org/10.1038/ki.2008.662

Tran, P. V., Talbott, G. C., Turbe-Doan, A., Jacobs, D. T., Schonfeld, M. P., Silva, L. M., Chatterjee, A., Prysak, M., Allard, B. A., & Beier, D. R. (2014). Downregulating hedgehog signaling reduces renal cystogenic potential of mouse models. *Journal of the American Society of Nephrology: JASN*, *25*(10), 2201–2212. https://doi.org/10.1681/ASN.2013070735

Wolf, M. T. (2015). Nephronophthisis and related syndromes. *Current Opinion in Pediatrics*, *27*(2), 201–211. https://doi.org/10.1097/MOP.0000000000000194

Zhang, H., Su, B., Liu, X., Xiao, H., Ding, J., & Yao, Y. (2018). Mutations in TTC21B cause different phenotypes in two childhood cases in China. *Nephrology (Carlton, Vic.)*, *23*(4), 371–376. https://doi.org/10.1111/nep.13008

Zhang, J., Sun, L., Kuang, X. Y., Kang, Y. L., Hao, S., Feng, D., Niu, X. L., & Huang, W. Y. (2022). Clinical phenotype analysis of 6 cases of TTC21B gene related nephronophthisis. *Zhonghua Er Ke Za Zhi*, *60*(8), 820–824. https://doi.org/10.3760/cma.j.cn112140-20211223-01076

How to cite this article: Li, Y., Dai, L., Xu, H., Huang, J., Zhang, J., Mei, Z., & Zhang, R. (2024). Clinical report and genetic analysis of rare premature infant nephronophthisis caused by biallelic *TTC21B* variants. *Molecular Genetics & Genomic Medicine*, *12*, e2399. https://doi.org/10.1002/mgg3.2399